

ADAPTIVE SLIDING MODE CONTROL FOR SHIP AUTOPILOT WITH SPEED KEEPING

Zhiquan Liu

Shanghai Maritime University, Shanghai, China

ABSTRACT

The paper addresses an important issue in surface vessel motion control practice that the ship dynamics and sailing performance can be affected by speed loss. The vessel speed is significantly decreased by the added resistance generated by waves. An adaptive sliding mode course keeping control design is proposed which takes into account uncertain ship dynamics caused by forward speed variations, while avoiding performance compromises under changing operating and environmental conditions. The sliding mode control provides robust performance for time-varying wave disturbances and time-varying changes in ship parameters and actuator dynamics. After combining the unknown but bounded system uncertainties, the design of the adaptation law is obtained which is based on the Lyapunov's direct method. Simulations on a ship with two rudders illustrate the effectiveness of the proposed solution.

Keywords: surface vessel; speed loss; adaptive control; course keeping; sliding mode control

INTRODUCTION

When a ship sails in a seaway, its maneuvering characteristics may be strongly affected by the ocean environment (i.e. waves, winds and currents). These environmental disturbances usually affect the ability of the ship to perform its mission, they may also cause cargo damage and produce variations of motion. The marine autopilot system is used to ensure sailing safety and to make the vessel navigate in the path by manipulating the rudder. The first autopilot mechanism was constructed in 1911, and the detailed theoretical analysis of proportional integral derivative (PID) controller for ship steering was presented by Nicholas Minorsky in 1922, when the yaw angle measurement was achieved using a gyrocompass [1]. The PID controller with fixed parameters can reveal good performance in particular operating conditions. However, the vessel dynamics can be affected by sailing conditions and external disturbances, i.e. loading, trim, forward speed and/or course variations, and the change of water depth under keel, which can decrease the quality of control of an autopilot with fixed gain.

Modern steering control systems focus on stability and performance robustness under the condition of uncertainties. The adaptive control probably stays as a good method to deal with this issue. The literature on ship autopilot control using adaptive and robust algorithms is widely surveyed, and a lot of studies have been published. In the area of the surface vessel path tracking control problem, the adaptive and backstepping techniques are combined to deal with unknown parameters and bounded time-varying external disturbances [2]. Zhang et al. [3] developed an adaptive neural network (NN) algorithm to capture system uncertainties and bounded wave disturbances under the condition of the unknown information on hydrodynamic structure. Shojaei [4] proposed a saturated tracking controller with NN and adaptive techniques to take into account unmodeled dynamics and to reduce the risk of actuator saturation. The above three methods are based on the passive bounded stable theory [5]. Peng et al. [6] developed two types of adaptive control methods, employing NNs and the DSC algorithm to track formations of autonomous surface vehicles. For course keeping of surface vessels, Do et al. [7] used the Lipschitz continuous projection

algorithm to estimate uncertainties which allowed to achieve the purpose of adaptive dynamics. Li et al. [8] adopted T-S fuzzy rules to deal with the model uncertainty problem for a nonlinear vehicle system. Kahveci and Ioannou [9] combined the adaptive law and the linear Quadratic (LQ) controller for uncertain ship dynamics with input constraints. The recurrent wavelet NN was employed as adaptive backstepping method to approximate the ideal backstepping law, and then to achieve a robust adaptive marine course changing control system [10]. For underwater vehicles, an adaptive robust controller was proposed for autonomous underwater vehicles (AUV) under changing operating conditions [11]. Do et al. [12] combined the backstepping and parameter projection methods to design a robust adaptive controller for AUV path following. An adaptive fuzzy NN method was introduced for trajectory tracking of an unmanned underwater vehicle (UUV) subject to stochastic bounded disturbances and parameter uncertainties [13].

Ships which advance with certain speed in open sea usually encounter large rate of motions due to ocean disturbances. Consequently, the total water resistance is increased by the added resistance, which may result in speed reduction and energy loss [14]. There is a survey that the magnitude of the added resistance is approximately equal to 10%–30% of the resistance in still water [15]. This added resistance worsens fuel efficiency and energy conservation, which are important issues from the commercial standpoint driven by business requirements in the marine industry [16]. In the area of ship motion control, the related work about the relationship between rolling and added resistance have been done by Liu and Jin [17]. They provided a practical PID method to design an optimal added resistance fin stabilizer controller. Yawing motion also increases the added resistance in waves, like the yawing motion caused by steering in still water [18]. Akinal [19] developed a kind of fuel saving steering control method to minimize propulsion losses. Grumble and Katebi [20] extended the LQG controller to minimize the energy loss caused by the added resistance induced by steering in ship course keeping control. Milon and Pachter [21] considered speed reduction in the collision avoidance control system. Kim et al. [22] studied ship's speed variations under different rudder controllers. The results recorded by them show that the ship speed in regular waves may be improved by decreasing the rudder rotation speed. Liu et al. [23] considered the resistance increase both in waves and in still water, and addressed a rudder roll stabilization (RRS) controller with speed reduction minimization. The control system designs presented in all above works act only under the condition of the ship moving with certain speed and ship dynamics unaffected by speed changes. However in practice, model parameter changes of the ship sailing in open seas are observed due to changes in ship speed. The forward speed is time varying because of the speed loss, which may lead to changes in vessel dynamics and control parameters. This paper aims to develop an adaptive ship autopilot controller with forward speed maintenance, which will consider unknown stochastic wave disturbances and parameter uncertainties caused by ship speed reduction.

The remaining part of the paper is organized as follows. Section 2 introduces the mathematical model, while the control algorithms are presented in Section 3. Simulation results are discussed in Section 4 and conclusions are drawn in Section 5.

Notations. Let \bullet be a scalar, a vector, or a matrix. $\|\bullet\|$ denotes the Euclidean norm when it is a vector or a matrix. $|\bullet|$ denotes the absolute value when it is a scalar.

PROBLEM FORMULATION

MATHEMATICAL MODEL OF SHIP

The model of ship sway-yaw dynamics has been introduced by Perez [25]. The main parameters of the ship are listed in Table 1.

$$m(\dot{v} + ur) + mx_G \dot{r} = Y_{\text{hyd}} + Y_c \quad (1)$$

$$mx_G(\dot{v} + ur) + I_{zz} \dot{r} = N_{\text{hyd}} + N_c \quad (2)$$

where m is the ship mass, I_{zz} is the inertia of the ship along the z-axis, and x_G is the coordinate of the center of gravity with respect to the body fixed frame. Surge and sway velocity components are denoted by u and v , respectively. ψ and r are the yaw angle and the yaw rate, while Y and N are the sway force and the yaw moment, respectively. Subscript hyd and c refer to the hydrodynamic term and to the control force produced by the actuator, respectively.

Tab. 1. Main parameters of the ship

Length (m)	52.50
Breadth (m)	8.80
Draft fore (m)	2.32
Draft aft (m)	2.26
Displacement volume (m ³)	355.88
Keel to transverse metacenter (m)	4.83
Keel to buoyancy (m)	3.34
Rudder area (m ²)	1.50

The hydrodynamic model equations are given as follows:

$$Y_{\text{hyd}} = Y_{\dot{v}} \dot{v} + Y_{\dot{r}} \dot{r} + Y_{|u|v} |u|v + Y_{ur} ur + Y_{v|v} v|v| + Y_{v|r} v|r| + Y_{r|v} r|v| \quad (3)$$

$$N_{\text{hyd}} = N_{\dot{v}} \dot{v} + N_{\dot{r}} \dot{r} + N_{|u|v} |u|v + N_{|u|r} |u|r + N_{r|r} r|r| + N_{r|v} r|v| \quad (4)$$

The rudder is the actuator used for heading control. The corresponding control forces are written as:

$$Y_c = L_r = \frac{1}{2} \rho A_R C_L(\delta) U^2 \quad (5)$$

$$N_c = L_r LCG \quad (6)$$

where ρ is the water density, L_r and A_R are the lift force and the area of the rudder, respectively. $C_L(\bullet)$ denotes the lift coefficient which varies with the rudder angle δ . LCG is the distance from the center of gravity to the rudder stock.

Assumption 1. The position and rate measurements of the sway and yaw motions of the ship are available for feedback.

Assumption 2. The ship parameters and added masses: m , I_z , $Y_{\dot{v}}$, $Y_{\dot{r}}$, $N_{\dot{v}}$, $N_{\dot{r}}$ are known. The nonlinear damping coefficients: $Y_{|u|v}$, Y_{ur} , $Y_{v|r}$, $Y_{v|v}$, $Y_{r|r}$, $N_{|u|v}$, $N_{|u|r}$, $N_{r|r}$, $N_{r|v}$ are also known, but the ship dynamics (damping matrix in the ship state-space model) depend on the ship forward speed.

Assumption 3. The ship control system based on the state-space model starts with the initial value of all parameters equal to zero.

Assumption 4. The surge dynamics is much slower than that in other motions, consequently the variable u is assumed equal to the ship moving speed U and satisfies: $0 < u_{\min} \leq |u(t)| \leq u_{\max}$ and $|\dot{u}(t)| \leq \dot{u}_{\max}$.

Assumption 5. The ship forward speed $U(t) = U_0 + \Delta U$ is time varying, where U_0 is the nominal (design) speed and ΔU is the time-varying speed loss which is unknown but bounded.

Remark 1. Several software packages and identification methods can be used to calculate or estimate ship parameters and added masses. For nonlinear damping terms, Perez [24] has modified the data of the selected vessel to match the load condition and main particulars. The main purpose in this paper is to study the effect of actual speed on ship dynamics and performance. Therefore, Assumption 3 is justified.

Remark 2. Assumption 5 means that the ship forward speed is nonzero and does not change sign.

Remark 3. In this paper, the calculation method presented by Liu et al. [23] is used to calculate the actual forward speed U and the speed loss ΔU .

The ship response to the control action is modelled using the linear model and assuming that $Y_c = Y_\delta \delta$ and $N_c = N_\delta \delta$. Then the model is expressed as:

$$(m - Y_{\dot{v}}) \dot{v} + (mx_G - Y_{\dot{r}}) \dot{r} = Y_{|u|v} Uv + Y_{ur} Ur - mUr + Y_\delta \delta \quad (7)$$

$$(mx_G - N_{\dot{v}}) \dot{v} + (I_{zz} - N_{\dot{r}}) \dot{r} = N_{|u|v} Uv + N_{ur} Ur - mx_G Ur + N_\delta \delta \quad (8)$$

Let us define the state-space model describing the ship linear heading control system. The unified model can be written using equations (7) and (8) as

$$\mathbf{M} \dot{\mathbf{v}} = \mathbf{D}(U) \mathbf{v} + \mathbf{H}(U) \delta \quad (9)$$

where the system states can be defined as $\mathbf{v} = [v, r, \psi]^T$, and the other matrices can be further represented as

$$\mathbf{M} = \begin{bmatrix} m - Y_{\dot{v}} & mx_G - Y_{\dot{r}} & 0 \\ mx_G - N_{\dot{v}} & I_z - N_{\dot{r}} & 0 \\ 0 & 0 & 1 \end{bmatrix} \quad (10)$$

$$\mathbf{D}(U) = \begin{bmatrix} Y_{|u|v} U & (Y_{ur} - m)U & 0 \\ N_{|u|v} U & (N_{|u|r} - mx_G)U & 0 \\ 0 & 0 & 1 \end{bmatrix} \quad (11)$$

$$\mathbf{H}(U) = \begin{bmatrix} 1 \\ -LCG \\ 0 \end{bmatrix} \frac{1}{2} \rho A_R U^2 \left. \frac{\partial C_L}{\partial \delta} \right|_{\delta=0} \quad (12)$$

It should be mentioned that the parameters in the damping matrix $\mathbf{D}(U)$ and in the control force matrix $\mathbf{H}(U)$ vary with the forward speed. Consequently, the dynamics of the ship and the actuator will be affected by the speed loss. This problem should be considered in the control system design addressed in the next section.

MATHEMATICAL MODEL OF WAVES

In this study, the long-crest wave spectrum model recommended by ITTC is utilized to simulate the waveforms of random waves. The desired spectrum model is given as:

$$S(\omega_i) = \frac{173 H_{1/3}}{T^4 \omega_i^5} \exp\left(-\frac{691}{T^4 \omega_i^4}\right) \quad (13)$$

where $H_{1/3}$ is the significant wave height, T is the wave period, and ω_i is the frequency of the i^{th} regular wave component.

To simulate random waves in the time domain, 60 regular waves were selected to form the irregular wave. The amplitude ζ_i of each regular wave component and the amplitude ζ of the resultant wave used to generate external forces and moments are given by the following expressions:

$$\zeta_i = \sqrt{2S(\omega_i) \Delta \omega} \quad (14)$$

$$\zeta = \sum_{i=1}^{60} \zeta_i \cos(\omega_i t + \varepsilon_i) \quad (15)$$

where ε_i is the random phase angle of the i^{th} regular wave.

Assumption 6. The disturbance signals of sway and yaw motions satisfy $|d_v(t)| \leq d_{v \max}$ and $|d_r(t)| \leq d_{r \max}$, where $d_{v \max}$ and $d_{r \max}$ are unknown positive constants.

ADDED RESISTANCE

The added resistance is independent of the calm water resistance. In this study, the added resistance produced by ship motions both in waves and in still water are considered.

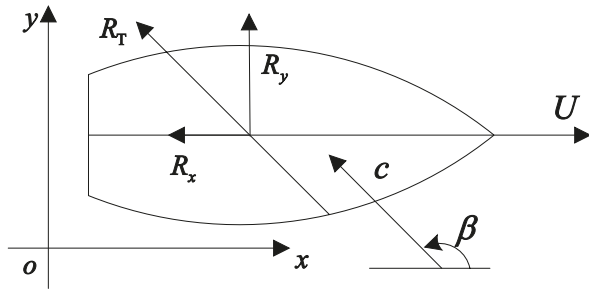


Fig. 1. Definition of added resistance and drift force

The method to calculate the added resistance in oblique waves is the extension of the radiated energy method proposed by Loukakis and Scavounos [25]. In Fig. 1, the ship is moving forward along a fixed direction. The waves are coming with propagation speed c at the encounter angle β . The horizontal force R_T can be resolved into two components: the added resistance R_x and the drift force R_y .

According to the radiated energy theory, the work of the added resistance is assumed to equate the energy of waves radiated away per wave period. With the strip theory approximations, the work of the horizontal force can be equated to the energy radiated away per encounter period. Consequently, the work passed to the fluid is given as follows:

$$P = (-R_T)(-c - U \cos \beta)T_e \quad (16)$$

where T_e is the encounter period.

Since the actuator is the rudder and only horizontal motions are included in this study, then the energy radiated by the horizontal motions are given by the following equations:

$$P_4 = \frac{\pi}{\omega_e} \int_L b_4 |p|^2 dx \quad (17)$$

$$P_{24} = P_{42} = \frac{\pi}{\omega_e} \int_L b_{24} |p U_{RY}| dx \quad (18)$$

$$P_{26} = \frac{\pi}{\omega_e} \int_L b_{26} |U_{RY}|^2 dx \quad (19)$$

where ω_e is the encounter frequency, L is the ship length, b is the motion damping coefficient, and the numerical subscripts represent their corresponding DOFs. U_{RY} is the transverse relative speed. Finally, the added resistance and the drift force in oblique waves can be written as:

$$(-R_T)(-c - U \cos \beta)T_e = P_4 + 2P_{24} + P_{26} \quad (20)$$

$$|R_x| = |R_T \cos \beta| \quad (21)$$

$$|R_y| = |R_T \sin \beta| \quad (22)$$

where P_4 , P_{24} and P_{26} are the energy amounts radiated by roll motion, yaw-roll motion, and sway-yaw motion, respectively, during one encounter period. The roll motion is not included when calculating the added resistance.

When the ship sails in calm water, the yaw angle caused by steering will produce pressure difference between its port and starboard sides. This kind of pressure difference creates extra resistance, referred to as the added resistance in calm water, discussed by Faltinsen [18].

The surge model in the body fixed frame is given as:

$$M(\dot{u} - vr) = X_{\dot{u}}\dot{u} - R_T(u) + (1 - \tau)T(u, n) + X_{vv}v^2 + X_{vr}vr + X_{rr}r^2 + X_{\delta\delta}\delta^2 \quad (23)$$

where $X_{\dot{u}}$, X_{vv} ,... are used to express longitudinal hydrodynamic forces acting on the hull and on the rudder. $R_T(u)$ is the ship calm resistance, τ is the thrust deduction coefficient, and $T(u, n)$ is the propeller revolutions per second.

The main cause of resistance increase is represented by Mvr and $X_{vr}vr$, while $R_T(u)$ and $T(u, n)$ are independent of the turning motion. The values of X_{vv} and X_{rr} are equal to zero when the surface vessel is symmetrical. The term $X_{\delta\delta}\delta^2$ is the extra drag due to rudder angle and can be neglected because of its small value.

Finally, the added resistance caused by yaw motion can be simplified to the form:

$$R_{yaw} = (M + X_{vr})vr \quad (24)$$

where M is the ship mass. This resistance is decided by sway rate and yaw rate.

CONTROL SYSTEM

The total speed loss in the heading control system is determined by the sway rate v and the yaw rate r . In the meanwhile, the heading error must be limited, therefore the three variables v , r , and ψ should be simultaneously constrained. The proposed autopilot system is shown in Fig. 2. Here, ψ_d is the desired heading angle and d is the external disturbance. The other desired values are set equal to zero. The saturation block is adopted to constrain the rudder angle amplitude.

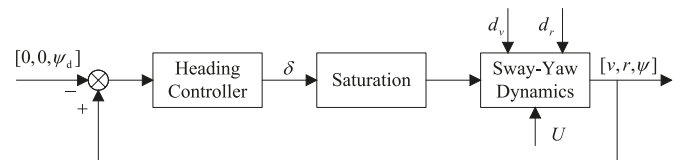


Fig. 2. The autopilot control system

The sliding mode control (SMC) used here can accommodate system parameter uncertainties and reject unknown bounded disturbances, as well as quantify the modeling and performance trade-off. Liu et al. [23] adopted the SMC method to design an RRS control system with forward speed minimization which assumed U as a constant design speed in the ship model. However, the actual forward speed varies in the time domain due to speed losses, which can cause uncertainties in the dynamics of ship and actuator,

and, consequently, decrease the robustness of the SMC. To improve the performance of the controller when the speed is time varying, an adaptive sliding mode control (ASMC) method has been selected. The following sections present the design process of the two controllers.

SLIDING MODE CONTROL DESIGN

In this section, the eigenvalue decomposition method is applied to provide an appropriate scheme to select weighting factors for the sliding surface function [1]. Assuming that the ship dynamics parameters are not affected by speed loss, the value of the parameter U in the ship model is equal to the nominal speed U_0 . After combining the wave disturbance terms, the state-space model (9) is transformed to the form:

$$\dot{\mathbf{x}} = \mathbf{A}\mathbf{x} + \mathbf{b}\delta + \mathbf{d}$$

where \mathbf{d} is bounded as $\|\mathbf{d}\| \leq d_{\max} < \infty$, and the detailed description is regarded as follows:

$$\begin{bmatrix} \dot{v} \\ \dot{r} \\ \dot{\psi} \end{bmatrix} = \begin{bmatrix} a_{11} & a_{12} & 0 \\ a_{21} & a_{22} & 0 \\ 0 & 1 & 0 \end{bmatrix} \begin{bmatrix} v \\ r \\ \psi \end{bmatrix} + \begin{bmatrix} b_1 \\ b_2 \\ 0 \end{bmatrix} \delta + \begin{bmatrix} d_v \\ d_r \\ 0 \end{bmatrix} \quad (25)$$

By choosing a suitable control law, the sliding manifold is used in the state error space to find the relationship for each control element. Let the reference state be $\mathbf{x}_d = [0, 0, \psi_d]$, and the sliding surface be defined as:

$$s = \mathbf{h}^T \mathbf{x}_e = \mathbf{h}^T (\mathbf{x} - \mathbf{x}_d) \quad (26)$$

where $\mathbf{h} = [h_1, h_2, h_3]^T$ is the right eigenvector of \mathbf{A}_c (i.e. $\mathbf{A}_c^T \mathbf{h} = \lambda \mathbf{h}$). The weighting vector is selected by computing the characteristic equation $\mathbf{A}_c^T \mathbf{h} = 0$ for $\lambda = 0$.

In the SMC system, the state feedback control law that limits ship motion responses is defined. In this case, the rudder angle command is separated into two parts,

$$\delta = \delta_0 + \delta_s \quad (27)$$

where $\delta_0 = -\mathbf{k}^T \mathbf{x}$ is the state feedback control law, which can also be an equivalent controller.

Substituting the control (27) into the equation (25), we obtain

$$\dot{\mathbf{x}} = \mathbf{A}_c \mathbf{x} - \mathbf{b}\delta_s + \mathbf{d} \quad (28)$$

where the combined state matrix is $\mathbf{A}_c = \mathbf{A} - \mathbf{b}\mathbf{k}^T$. The feedback gain vector is defined as $\mathbf{k} = [k_1, k_2, 0]^T$ to stabilize the sway-yaw dynamics. Here, $k_3 = 0$ due to integration in the yaw channel.

The nonlinear control part δ_s is the switching law which counteracts the destabilizing effects of environmental disturbances. It is written as:

$$\delta_s = -(\mathbf{h}^T \mathbf{b})^{-1} \eta \operatorname{sgn}(s) \quad (29)$$

where the switching gain satisfies $\eta > d_{\max} \|\mathbf{h}\|$.

Differentiating the sliding surface manifold, we arrive at:

$$\begin{aligned} \dot{s} &= \mathbf{h}^T \mathbf{A}_c \mathbf{x} + \mathbf{h}^T \mathbf{b}\delta_s + \mathbf{h}^T \mathbf{d} - \mathbf{h}^T \dot{\mathbf{x}}_d \\ &= \lambda \mathbf{x}^T \mathbf{h} - \eta \operatorname{sgn}(s) + \mathbf{h}^T \mathbf{d} \end{aligned} \quad (30)$$

where $\lambda \mathbf{x}^T \mathbf{h} = 0$ if \mathbf{h} is the right eigenvector, and $\mathbf{h}^T \dot{\mathbf{x}}_d = 0$.

To prove the stability of the closed loop system, the Lyapunov function is selected:

$$V = \frac{1}{2} s^2 \quad (31)$$

The differentiation of Equation (31) can be written as

$$\begin{aligned} \dot{V} &= s\dot{s} = -\eta \operatorname{sgn}(s)s + \mathbf{h}^T \mathbf{d} \\ &= -\eta |s| + \mathbf{h}^T \mathbf{d} \leq 0 \end{aligned} \quad (32)$$

The above equation indicates that the state trajectory can reach the sliding manifold in finite time and decline to zero. Consequently, the control law guarantees the sustainability of the sliding mode.

In order to attenuate the chattering effect, the *tanh* function is used in place of *signum* function. Hence, the total control law of autopilot becomes

$$\delta = -(k_1 v + k_2 r) - (h_1 b_1 + h_2 b_2)^{-1} \eta \tanh(s/\phi) \quad (33)$$

where ϕ is the boundary layer thickness.

ADAPTIVE SLIDING MODE CONTROL DESIGN

In practice, the dynamics of the ship and the actuator are affected by the time-varying speed, which is the source of parameter uncertainties. The upper bounds of disturbance and parameter uncertainties, and the value of η are often difficult to find. The uncertainties in the system are assumed to meet the matching conditions. In this section, the modified control law is presented. The purpose of the adaptive method is to tune the controller gain without the knowledge about the upper bound of system uncertainties.

Considering the speed $U(t) = U_0 + \Delta U$, varying with time due to speed loss, the system state-space model is written as

$$\dot{\mathbf{x}} = \mathbf{A}(U(t))\mathbf{x} + \mathbf{b}(U(t))\delta + \mathbf{d} \quad (34)$$

where the state matrix and the control matrix can be divided into the nominal part and the uncertain part:

$$\mathbf{A}(U(t)) = \mathbf{A} + \Delta \mathbf{A} \text{ and } \mathbf{b}(U(t)) = \mathbf{b} + \Delta \mathbf{b}$$

Then we obtain a new equation:

$$\dot{\mathbf{x}} = \mathbf{A}\mathbf{x} + \mathbf{b}\delta + \mathbf{E}(\Delta U, \mathbf{x}, \delta) \quad (35)$$

where $\mathbf{E}(\Delta U, \mathbf{x}, \delta) = \Delta \mathbf{A}\mathbf{x} + \Delta \mathbf{b}\delta + \mathbf{d}$ is the lumped uncertainty.

The modified control law developed here is

$$\delta_a = \delta_{a0} + \delta_{as} \quad (36)$$

where the linear feedback controller δ_{a0} is the same as δ_0 used in the nominal system.

Corresponding to the lumped uncertainty, the robust switching control part is modified as

$$\delta_{as} = -(\mathbf{h}^T \mathbf{b})^{-1} \hat{\eta}_a \operatorname{sgn}(s) \quad (37)$$

where $\hat{\eta}_a$ is the estimate of the adjustable gain. Assuming that there is a positive η_a for which $\delta_{as} = -(\mathbf{h}^T \mathbf{b})^{-1} \eta_a \operatorname{sgn}(s)$ is the terminal solution, the gain η_a must satisfy $\eta_a > \|\mathbf{h}^T\| \cdot \|\mathbf{E}(\Delta U, \mathbf{x}, \delta)\|$.

The adjustable gain can be tuned by the adaptation law defined as

$$\dot{\hat{\eta}}_a = \frac{1}{\alpha} |s| \quad (38)$$

where $\alpha > 0$ is the adaptation gain. Selecting a reasonable adaptation gain can effectively help to avoid high control activity. For simplicity, let it be a positive constant in this control system.

To avoid over increased estimate values of $\hat{\eta}_a$ that may lead to large amplitude control signal, this quantity should be limited in a suitable range. That is why the projection algorithm presented by Do et al. [2] is used to modify the adaptation law into the following

$$\dot{\hat{\eta}}_a = \operatorname{Proj}_{\hat{\eta}_a}(\dot{\hat{\eta}}_a) \quad (39)$$

$$\operatorname{Proj}_{\hat{\eta}_a}(\bullet) = \begin{cases} 0 & \text{if } \hat{\eta}_a \geq \eta_{\max} \text{ and } \bullet > 0 \\ 0 & \text{if } \hat{\eta}_a \leq \eta_{\min} \text{ and } \bullet < 0 \\ \bullet & \text{otherwise} \end{cases} \quad (40)$$

Theorem 1. For the system (26): Given the control law (36) and the eigenvector property in the equation (30), under Assumptions 1-6 the proposed adaptive control strategy can guarantee driving the state trajectories of the system onto the sliding surface in finite time.

Proof: Consider the same sliding surface function as in the above section. Then its differentiation is written as

$$\begin{aligned} \dot{s} &= \mathbf{h}^T \dot{\mathbf{x}}_e = \mathbf{h}^T \dot{\mathbf{x}} = \mathbf{h}^T (\mathbf{A}_c \mathbf{x} + \mathbf{b} \delta_{as} + \mathbf{E}) \\ &= \mathbf{h}^T \mathbf{b} \delta_{as} + \mathbf{h}^T \mathbf{E} \end{aligned} \quad (41)$$

Define the estimate error as $\tilde{\eta}_a = \hat{\eta}_a - \eta_a$, and choose a Lyapunov function candidate as

$$V = \frac{1}{2} s^2 + \frac{1}{2} \alpha \tilde{\eta}_a^2 \quad (42)$$

Multiplying both sides of Equation (41) by the sliding surface, the following equation is obtained

$$s \dot{s} = s(\mathbf{h}^T \mathbf{E} - \hat{\eta}_a \operatorname{sgn}(s)) = s \mathbf{h}^T \mathbf{E} - \hat{\eta}_a |s| \quad (43)$$

In the same way, the corresponding equation for the adaptation error is given as

$$\alpha \tilde{\eta}_a \dot{\tilde{\eta}}_a = \alpha (\hat{\eta}_a - \eta_a) \dot{\hat{\eta}}_a = (\hat{\eta}_a - \eta_a) |s| \quad (44)$$

Applying Equations (43) and (44), and taking the derivative of the Lyapunov function, we get

$$\dot{V} = s \dot{s} + \alpha \tilde{\eta}_a \dot{\tilde{\eta}}_a = s \mathbf{h}^T \mathbf{E} - \eta_a |s| \leq 0 \quad (45)$$

Hence, the convergence of s and $\tilde{\eta}_a$ is proven by the Lyapunov direct method, both s and $\tilde{\eta}_a$ reach zero in finite time. To alleviate the chattering phenomenon, the boundary layer method with *tanh* function can be used to replace *signum*, like in the description in the SMC design section. In the proposed ASMC scheme, the knowledge of the upper bound of system uncertainties is not required.

SIMULATION RESULTS

The simulation of the autopilot control system working on a navy vessel with speed keeping control is demonstrated. The nominal ship speed is 15 knots, the wave height is 3.7 m, and the average period is 7 s. The rudder angle limitation is 35° and two rudders are installed. The desired state trajectory is assumed to be $\mathbf{C}_d = (0, 0, 0)^T$, the initial state vector is $\mathbf{x} = (0, 0, 0)^T$ and the initial guess of η is $\eta = 5$. The adaptation law is set as $\alpha = 0.05$ and $\hat{\eta}_a(0) = 2.5$. The boundary layer is chosen as $\phi = 1$. The other parameters \mathbf{k} and η_{\min}, η_{\max} are set as $[10, 100, 0]^T$ and $(2, 25)$, separately. The ship is sailing with the encounter angle 120°.

Fig. 3 compares autopilot dynamics under the open-loop condition. The solid lines represent the time-histories of ship dynamics which consider the effect of time-varying speed loss, while the dashed lines mean the responses of the nominal ship model. The sway and yaw rate responses are identical for these two models. On the other hand, the yaw angle magnitude is increased under the action of time-varying ship dynamics which may generate ship course changes. The speed response is less declined, as the values of speed loss depend on sway and yaw rates, as presented by Liu et al. [24].

Tab. 2. Cost value of simulation

Controller	Yaw response	Average speed (Kn)	Rudder usage
SMC	1867.09	13.49	48927.57
ASMC	1590.05	13.73	58032.68

The results of ship's performance calculations with the two control methods are presented in Fig. 4. In the first graph, the response of the sway rate is not changed. Actually, the rudder control force for sway motion is *LCG* times smaller than that for yaw motion (compare equations (5) and (6)), therefore we can ignore this control force and assume it as an underactuated surface vessel. The proposed ASMC scheme can give better sailing performance, as the yaw motion and

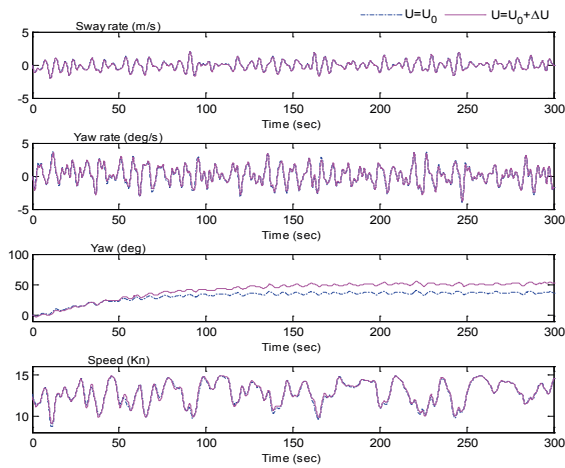


Fig. 3. Responses of the uncontrolled autopilot system

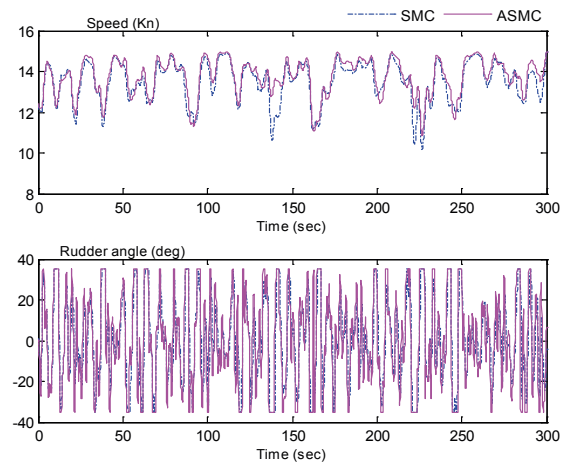


Fig. 5. Comparison of speed and rudder angles

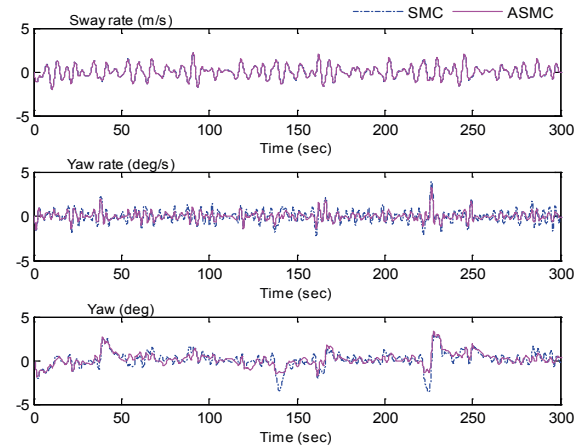


Fig. 4. Simulation results of sway and yaw

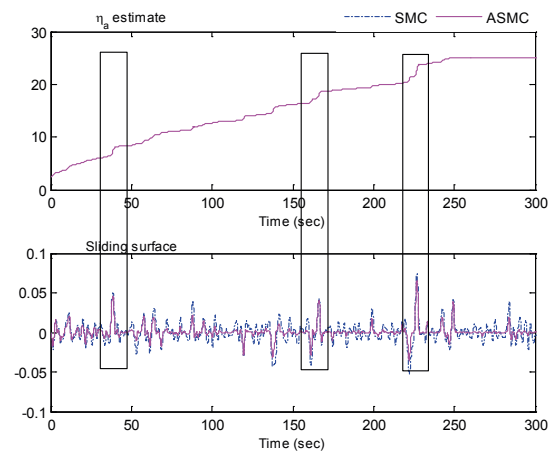


Fig. 6. Simulation results of adaptive trajectory and sliding surface controllers

its rate are both reduced to a greater extent than by the SMC method. That means that the speed loss (i.e. fuel consumption increase) can be reduced more. At the sea state for the case presented in Fig. 5, the reduction of speed loss percentage is 1.54%, which cannot be ignored in the real voyage of a ship. Fig. 5 also compares rudder orders. The adaptive controller may use a little more energy to drive rudders and cause rudder angle saturation. The values calculated from the cost function are listed in Table 2.

Fig. 6 presents the time-histories of the results obtained using the adaptive estimate and sliding surface controllers. The estimate value is continuously increasing, with stepwise increase at each corresponding peak in the sliding surface, marked by three rectangles in Fig. 6. This is because the adaptation law is substantially an integral function of the sliding surface. This is also the reason why the projection algorithm is adopted here to limit this value. This kind of varying estimate value generates more effective rudder control commands to reject system uncertainties due to speed loss and unknown disturbances.

CONCLUSIONS

In the paper, the problem of adaptive sliding mode control design for ship autopilot system with fuel efficiency control is studied. The control problem is formulated in a single-input-multiple-output framework with a time-varying ship model due to speed loss. The adaptation accounts for changes in ship speed to ensure that the appropriate drag forces are minimized. The paper also presents the responses of the rudders to changes in the seaway environment. The variations of parameters in the system and in the external disturbance are both robust, and the tracking capacity is guaranteed. The ASMC method can improve the heading control performance. What is more important, the actual sailing speed of the ship is significantly improved by the control system with respect to sailing energy consumption. Notably, the information on upper bounds of system uncertainties and wave disturbances is not required. When applying this strategy, the initial value set for the adaptation estimate should be smaller than the nominal upper bound. For the sake of safety, the projection

algorithm method is proposed to avoid an unexpected unlimited increase of the adaptation estimate. Simulation results have been provided to illustrate the effectiveness of the proposed approach.

REFERENCES

1. Fossen T.I.: *Handbook of marine craft hydrodynamics and motion control*. Wiley, West Sussex, 2011.
2. Do K.D., Jiang Z.P., Pan J.: *Robust adaptive path following of underactuated ships*. *Automatica*, vol. 40, no. 6, 929, 2004.
3. Zhang G., Zhang X., Zheng Y.: *Adaptive neural path following control for underactuated ships in fields of marine practice*. *Ocean Engineering*, no. 104, 558, 2015.
4. Shojaei K.: *Neural adaptive robust control of underactuated marine surface vehicles with input saturation*. *Applied Ocean Research*, no. 53, 267, 2015.
5. Li J.H., Lee P.M., Jun B.H., Lim Y.K.: *Point to point navigation of underactuated ships*. *Automatica*, vol. 44, no. 12, 3201, 2008.
6. Peng Z., Wang D., Chen Z., Hu X., Lan W.: *Adaptive dynamic surface control for formations of autonomous surface vehicles with uncertain dynamics*. *IEEE Transactions on Control System Technology*, vol.21, no. 2, 513, 2013.
7. Do K.D., Pan J., Jiang Z.P.: *Robust adaptive control of underactuated ships on a linear course with comfort*. *Ocean Engineering*, vol. 30, no. 7, 2201, 2003.
8. Li H., Liu J., Hilton C., Liu H.: *Adaptive sliding mode control for nonlinear active suspension vehicle systems using T-S fuzzy approach*. *IEEE Transactions on Industrial Electronics*, vol. 60, no. 8, 3328, 2013.
9. Kahveci N., Ioannou P.A.: *Adaptive steering control for uncertain ship dynamics and stability analysis*. *Automatica*, vol. 49, no. 3, 685, 2013.
10. Lin C., Hsuen C., Chen C.: *Robust adaptive backstepping control for a class of nonlinear systems using recurrent wavelet neural network [J]*. *Neurocomputing*, no. 142, 372, 2014.
11. Cristi R., Papoulias F.A., Healey A.J.: *Adaptive sliding mode control of autonomous underwater vehicles in the dive plane*. *IEEE Journal of Oceanic Engineering*, vol. 15, no. 3, 152, 1990.
12. Do K.D., Pan J., Jiang Z.P.: *Robust and adaptive path following for underactuated autonomous underwater vehicles*. *Ocean Engineering*, vol. 31, no. 6, 1967, 2004.
13. Liu Y., Liu S., Wang N.: *Fully tuned fuzzy neural network robust adaptive tracking control of unmanned under water vehicle with thruster dynamics*. *Neurocomputing*, no. 196, 1, 2016.
14. Prpic-Orsic J., Faltinsen O.M.: *Estimation of ship speed loss and associated CO2 emissions in a sea way*. *Ocean Engineering*, vol. 44, no. 1, 1, 2012.
15. Arribas F.P.: *Some methods to obtain the added resistance of a ship advancing in waves*. *Ocean Engineering*, vol. 34, no. 7, 946, 2007.
16. Armstrong V.N.: *Vessel optimisation for low carbon shipping*. *Ocean Engineering*, no. 73, 195, 2013.
17. Liu Z., Jin H.: *Extended radiated energy method and its application to a ship roll stabilisation control system*. *Ocean Engineering*, vol. 72, no. 7, 25, 2013.
18. Faltinsen O.M.: *Hydrodynamics of High Speed Vehicles*. Cambridge University Press, Cambridge 2005.
19. Akinsal V.: *Surface ship fuel saving with an optimized autopilot, master dissertation*. Naval Postgraduate School, Monterey, 1985.
20. Grimble M.J., Katabi M.R.: *LQG design of ship steering control systems*. *Signal Processing for Control, Lecture Notes in Control and Information Sciences*, no. 79, 387, 1986.
21. Miloh T., Pachter M.: *Ship collision-avoidance and pursuit-evasion differential games with speed-loss in a turn*. *Computers Mathematics with Application*, vol. 18, no. 1, 77, 1989.
22. Kim S.S., Kim S.D., Kang D., Lee J., Lee S.J., Jung K.H.: *Study on variation in ship's forward speed under regular waves depending on rudder controller*. *International Journal of Naval Architecture and Ocean Engineering*, vol. 7, no. 2, 364, 2015.
23. Liu Z., Jin H., Grimble M.J., Katebi R.: *Ship forward speed loss minimization using nonlinear course keeping and roll motion controllers*. *Ocean Engineering*, no. 113, 201, 2016.
24. Perez T.: *Ship Motion Control: Course Keeping and Roll Reduction Using Rudder and Fins*. Springer, London, 2005.
25. Loukakis T.A., Sclavounos P.: *Some extensions of the classical approach to strip theory of ship motion including the calculation of mean added forces and moments*. *Journal of Ship Research*, vol. 22, no. 1, 1, 1978.

CONTACT WITH THE AUTHOR

Zhiquan Liu

e-mail: liuzhiquan215@sina.com

Shanghai Maritime University

1550 Haigang AVE

201306 Shanghai

CHINA